

Optimization of Geotechnical Material Proportion and Forecast of Mechanical Properties Based on Neural Network

Kaicheng Liu^{1,*}, Rui Guo¹, Rongchuan Liu², Honglei Qiao³

¹Wuhan University of Technology, Wuhan, China

²Hefei University of Technology, Hefei, China

³Shandong University, Jinan, China

*Corresponding Author.

Abstract:

With the rapid development of economic construction and the rapid development of rock engineering, it is very important to study the mechanical properties of rock mass. This paper prepares the geotechnical materials and finds out the factors that affect the geotechnical properties. In order to reasonably match the rock materials and find the optimal solution, this paper transforms the multi-factor ratio optimization problem into a multi-factor linear optimization problem. By constructing a multiple regression equation, and using the genetic algorithm to solve the multivariate optimization of the objective function, a suitable matching scheme is found. Then, this paper predicts the mechanical properties of the rock, and uses neural network to predict the shear strength of the rock, and establishes an optimization structure to verify the model. The results show that the error of the ratio optimization scheme adopted in this paper is less than 2%, and the forecast scheme of mechanical properties is less than 18%, which has certain reference significance.

Keywords: Genetic algorithm; Neural network; Orthogonal experiment; Rock; Shear strength

I. INTRODUCTION

1.1 Research Background and Significance

Entering the 21st century, China's economic construction has continued to advance, and large-scale construction has spread throughout the country. In the construction of roads, bridges and water conservancy engineering facilities, it is necessary to face the complex and changeable geotechnical environment. In order to speed up the industrialization process and classify the geotechnical materials, it is of great significance to study the mechanical properties of the rock mass surface.

Rock as an engineering material is widely used in construction, and due to the different components of rock and soil, the different mechanical strength and damage resistance will directly affect the quality of rock engineering construction. However, due to the insufficiency of the current technology, the current research on the mechanical properties of rocks cannot achieve a major breakthrough in a short period of time. It has

been proved by experiments that experiments and analysis of rock and soil can reflect the mechanical properties of rock mass and the failure process of rock mass[1]. The destructive properties and shear deformation of rock and soil have very important engineering value for engineering construction and danger warning.

In the large-scale outdoor reset experiment, although the real geotechnical properties and the failure process of the rock mass can be simulated, this method requires a large amount of resources and the experiment period is very long, and the acquisition experiment is restricted by the natural weather. Compared with large-scale outdoor reset experiments, indoor physical experiments are not affected by natural weather and can simulate experiments under macro-controllable conditions. Therefore, the indoor simulation method is widely recognized in academia.

Because the brittleness of the rock is obvious, the material ratio of the rock can be simulated by studying the mechanical properties of the rock. Therefore, in this paper, the target rock material is determined by simulating pairing of rocks with similar brittle characteristics. Since the proportioning scheme is the most important link in the study of mechanical properties of similar materials, the optimal design of the proportioning scheme is one of the research focuses of this paper. The stability of rock mass engineering depends on the shear mechanical properties of rock and soil. However, due to the complex structure and various shapes of rock and soil, it is difficult to detect the shear mechanics of rock and soil, and it is difficult to establish a theoretical model for accurate detection. Due to the advantages of neural network in dealing with nonlinear relationship and its special feature extraction method, neural network is widely used in geotechnical mechanics. Therefore, it is of great significance to predict the mechanical properties of rock and soil joints using neural networks.

In this paper, genetic algorithm is selected to optimize the proportion of rock-like materials. In this paper, the optimization algorithm scheme is constructed, the results are verified and compared, and the shear strength of rock and soil is predicted and analyzed by neural network.

1.2 Research Status

1.2.1 Research on rock materials

Scholars have conducted many experiments and researches on the properties of rock-like materials. In recent years, domestic scholars have used orthogonal design to study and analyze the influence of multiple factors on the mechanical properties of rock-like[2]. Some scholars have used 3D printing technology to analyze the material mechanical properties of rock masses[3]. The influence of confining pressure on the mechanical properties of rock materials was studied[4]. Foreign scholars such as M. Prudencio verified the failure characteristics of rock-like physical models through failure simulation experiments[1], and YJ Cao carried out macroscopic material mechanical properties analysis of rock-like materials with voids by establishing multi-scale rock-like models[5], Zizi Pi proposed to use computer technology to describe the properties of rock materials by remote sensing[6]. It can be seen from the above that indoor physical simulation experiments can be used as a method to study the characteristics of rock materials.

1.2.2 The status quo of ratio optimization

In the past 100 years, scholars at home and abroad have conducted time and again research on the ratio factors of rock-like materials. The traditional ratio optimization method is designed by experience, so its limitations are prominent. When the mechanical characteristics of the rock are not obvious or the internal structure of the rock is changed due to weathering and erosion, the traditional empirical judgment is seriously limited. The emergence of modern neural network has brought new design ideas for the optimization of rock mass material ratio.

In recent years, neural networks and genetic algorithms have been widely used in the field of engineering construction design, and more and more scholars have also applied neural networks and genetic algorithms to the optimization of the proportion of geotechnical materials. Chinese scholars established a mathematical model through the genetic algorithm optimization design tool of MATLAB and the quadratic programming method to optimize the design of the proportioning and filling of concrete[7]. Chinese scholars use the orthogonal experiment method to design by combining the neural network technology into the ratio optimization of the mixture[8]. Soon after, Chinese scholars designed a high-precision mathematical model, using genetic algorithm to achieve multi-objective optimization of concrete frost resistance and concrete cost[9].

It can be seen from the above that the ratio optimization of the neural network and the genetic algorithm has relatively considerable optimization results. Therefore, in this paper, the proportion of geotechnical materials is optimized, and the optimization results are analyzed.

1.2.3 Research status of shear mechanical properties of rock joints

As early as 1973, foreign scholar Barton[10] proposed the joint roughness coefficient, namely *JRC* (joint roughness coefficient), using field observation and multiple experiments, and proposed ten contour lines of *JRC* in [0, 20]. Scholars at home and abroad have conducted many studies and discussions on the shear mechanical properties of rock and soil. Sayles and Thomas[11] proposed the characteristics of contour lines in 1977, namely *CLA* (center line mean), *RMS* (root mean square value), *SF*(structure function), *Z2*(first derivative root mean square), *Z3* (Second derivative root mean square), *Z4* (third derivative root mean square). Subsequently, scholars used *R_p* to define the roughness of the joint outline, and established the structural relationship between *SF*, *Z2* and *JRC*, as shown in equations (1) and (2). Scholars calculated the relationship between *R_p* and *JRC* through experiments in 1990, as shown in formula (3).

$$JRC = 32.2 + 32.47 \log_{10} Z_2 \quad (1)$$

$$\begin{aligned} JRC \\ = 37.28 + 16.58 \log_{10} SF \end{aligned} \quad (2)$$

$$JRC = 411(R_p - 1) \quad (3)$$

A large number of theoretical studies have found that the shear mechanical properties of rock joints are

affected by a variety of factors. In 1997, Chinese scholars proposed a method to predict rock mass mechanics using neural network[12]. In the 21st century, with the gradual rise of neural networks, in 2002, foreign scholars used BP neural network to predict and analyze the friction angle and cohesion in the shear strength of rock-soil joints[13]. In recent years, some scholars proposed to use optimization algorithms and neural networks to predict and analyze the peak shear strength, which brought hope for the analysis of rock shear mechanics.

To sum up, the theoretical mathematical model cannot predict and analyze the shear mechanical properties of rock joints. The BP neural network studied in this paper can predict the shear mechanical properties and improve the accuracy and stability of the prediction, which is in line with the current social research hotspots.

II. RESEARCH ON THE PROPERTIES OF GEOTECHNICAL MATERIALS

2.1 Selection of Materials

Since the water content in the river sand is less than 2%, and the fineness modulus is less than 3.1, the river sand is easy to obtain and easy to screen. In this paper, river sand is selected as the aggregate of the rock-like material, gypsum is selected as the cementitious material, and an appropriate amount of iron powder is added to improve the strength of the rock-like material.

2.2 Experimental Design

2.2.1 Scheme design

Orthogonal experimental design establishes a standardized orthogonal table through probability theory, statistics and experimental experience, and can deal with multi-factor optimization problems by arranging different experimental factors to conduct combined experiments. The experimental scheme designed in this paper is shown in Table I and Table II.

TABLE I. Screening of experimental factors

Group	Water-to-paste ratio	Iron content/%	Sand content/%
1	0.44	1.5	13.2
2	0.46	2	15.6
3	0.48	2.5	18
4	0.50	3	20.4
5	0.52	3.5	22.8

TABLE II. Orthogonal experimental design scheme

Group	Water-to-paste ratio	Iron content/%	Sand content/%
1	0.44	2.5	18
2	0.44	2.0	15.6
3	0.46	2.5	13.2
4	0.48	1.5	15.6
5	0.5	2.5	15.6
6	0.48	3.5	13.2
7	0.48	2.5	20.4
8	0.5	3	18
9	0.52	3	13.2
10	0.46	3	15.6
11	0.48	3	22.8
12	0.50	1.5	22.8
13	0.52	2	20.4
14	0.52	2.5	22.8
15	0.46	3.5	18
16	0.44	3.5	15.6
17	0.44	3	20.4
18	0.44	3.5	22.8
19	0.44	1.5	13.2
20	0.50	3.5	20.4
21	0.52	1.5	18
22	0.46	2	22.8
23	0.48	2	18
24	0.50	2	13.2
25	0.46	1.5	20.4

2.2.2 Sample making and selection

Before making the sample, make a mold in advance. The bottom of the cylindrical grinding tool is $\Phi 40$, the height is 80 mm, and the square grinding tool is 80 mm \times 80 mm \times 80 mm, as shown in Figure 1(a) and Figure 1(b).

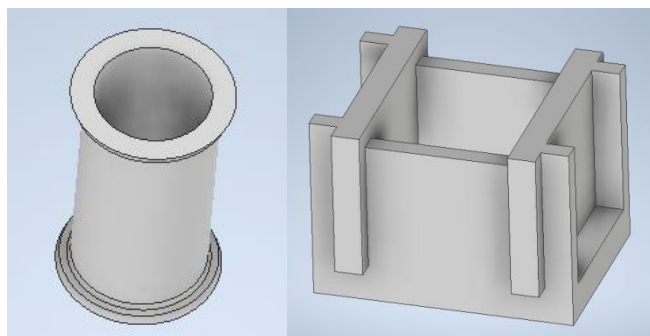


Fig 1: Round mold (left. a) and square mold (right. b)

The production is carried out in accordance with the standard sample production method, which will not be repeated in this article. After the production is completed, the flatness of the sample should be ground. The SHM-200 double-end grinding stone machine shown in Figure 2 can grind the end surface. Subsequently, the samples with better loaded end faces and the flatness of the end faces less than 0.1 mm were selected as optional experimental samples, and the flatness of the end faces could be measured by a flatness measuring instrument.



Fig 2: SHM-200 double-end grinding stone machine

2.3 Testing of Mechanical Properties

In this experiment, the above orthogonal experimental designs are matched. In this paper, the Brazilian splitting experiment, uniaxial compression experiment, triaxial compression experiment and direct shearing experiment will be used to compare, so as to obtain the mechanical parameters of each group. The four experiments are as follows.

2.3.1 Uniaxial compression experiment

The three mechanical parameter values of σ_c (compressive strength), E (modulus of elasticity), and ν (Poisson's ratio) are obtained through uniaxial compression experiments, and uniaxial compression experiments are carried out using TAW-2000 electro-hydraulic rock triaxial testing machine. In the experiment, the calculation formulas of compressive strength, elastic modulus and Poisson's ratio are as follows.

$$\sigma_c = \frac{P}{A} \quad (4)$$

$$E = \frac{\sigma_c}{\varepsilon_a} \quad (5)$$

$$\nu = \frac{\varepsilon_r}{\varepsilon_a} \quad (6)$$

Among them, P is the peak load (KN), A is the load surface area (mm²), ε_a is the axial strain, and ε_r is the radial strain.

2.3.2 Brazilian splitting experiment

The Brazilian splitting test can obtain the peak load during splitting. The value of σ_t can be obtained according to the calculation method of tensile strength. The calculation method is as follows.

$$\sigma_t = \frac{2P}{\pi Dh} \quad (7)$$

In the experiment, the displacement curve is shown in Figure 3. It can be seen from the image that the initial stress of the sample grows slowly, and then undergoes a short elastic stage, and cracks appear at half the peak stress level. When the ultimate load is reached, the load capacity of the sample increases. decline rapidly.

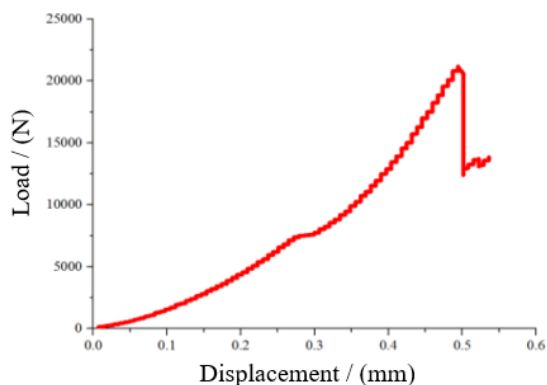


Fig 3:Stress-displacement curve

2.3.3 Direct shear test

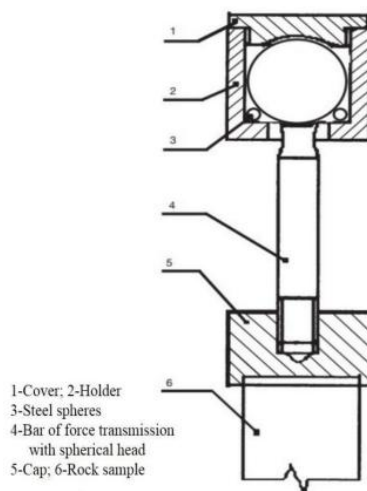


Fig 4: Direct shear experimental setup

The experimental process of direct shearing is shown in Figure 4, and the size of τ_f can be calculated by the experiment. The calculation process is as follows.

$$\tau_f = \frac{V}{A} = \frac{V}{b(h-s)} \quad (8)$$

Among them, V is the peak load (KN) when the sample fails; A is the sheared cross-sectional area of the sample (mm^2); b is the width of the sample cross-section (mm); h is the length of the sample cross-section (mm); s is the transverse direction Deformation (mm).

2.3.4 Triaxial compression experiment

Through the triaxial compression experiment, the maximum failure strength of the sample under different pressures can be obtained, and the Mohr stress circle and the strength envelope can be drawn. According to the Mohr-Coulomb strength formula as follows, the shear strength values c and φ can be obtained.

$$\tau = c + \sigma \tan \varphi \quad (9)$$

Assuming $k = \sigma_t / \sigma_c$, σ_t is the tensile strength, σ_c is the compressive strength, so the shear strength parameters of rock-like materials can be calculated, and the calculation process is as follows. The values of c and φ refer to formula 10 and 11.

$$\tan \varphi = \frac{1-k}{2\sqrt{k}} \quad (10)$$

$$c = \frac{\sigma_t}{2\sqrt{k}} = \frac{\sqrt{k}}{2} \sigma_c \quad (11)$$

After the above experiments, the mechanical parameter values of 25 groups of experiments can be determined, as shown in Table III.

TABLE III. Calculated values of mechanical parameters

Group	σ_c /Mpa	σ_t /Mpa	τ_f /Mpa	E/Gpa	ν	$\phi/^\circ$	c/Mpa
1	21.08	1.37	5.61	8.89	0.014	59.63	2.98
2	18.95	1.32	5.41	8.06	0.024	59.60	2.78
3	18.56	1.19	5.42	8.82	0.06	59.32	2.60
4	16.78	1.04	4.45	7.08	0.08	57.48	2.10
5	18.26	1.09	4.20	6.36	0.10	58.16	2.25
6	17.85	1.17	5.20	7.90	0.09	58.58	2.44
7	16.80	1.20	5.21	6.21	0.05	58.61	2.59
8	16.70	1.15	4.35	6.20	0.11	58.26	2.39
9	15.20	1.07	3.42	6.70	0.12	57.64	2.20
10	19.14	1.25	5.50	8.24	0.07	58.62	2.66
11	15.89	1.11	4.52	5.99	0.67	57.92	2.31
12	14.71	0.97	3.99	6.48	0.11	58.53	2.07
13	15.13	0.98	2.66	4.98	0.13	58.46	2.14
14	14.81	1.06	3.17	5.36	0.16	58.62	2.21
15	20.42	1.26	5.14	6.46	0.08	59.23	2.69
16	15.84	1.11	3.64	5.32	0.18	59.06	2.24
17	20.40	1.40	5.66	7.42	0.04	58.22	2.88
18	20.66	1.43	6.12	6.46	0.06	58.27	2.87
19	18.96	1.19	5.26	8.41	0.05	59.64	2.52
20	18.01	1.20	4.12	6.98	0.14	58.37	2.33
21	14.87	1.02	2.24	5.16	0.18	58.26	1.96
22	17.86	1.11	5.22	5.61	0.08	59.11	2.4
23	17.36	1.08	5.13	6.23	0.09	58.78	2.24
24	16.68	1.00	4.24	5.69	0.11	59.26	2.53
25	17.58	1.09	5.23	7.68	0.08	59.47	2.40

III. PROPORTION OPTIMIZATION ALGORITHM

3.1 Genetic Algorithm

Genetic algorithm is an artificial intelligence technology that simulates biological evolution with the idea of biological evolution as the core. With the continuous improvement of the genetic algorithm in the scientific community, the current genetic algorithm can solve the optimization problem of multiple factors. The operation steps of the genetic algorithm are shown in Figure 5.

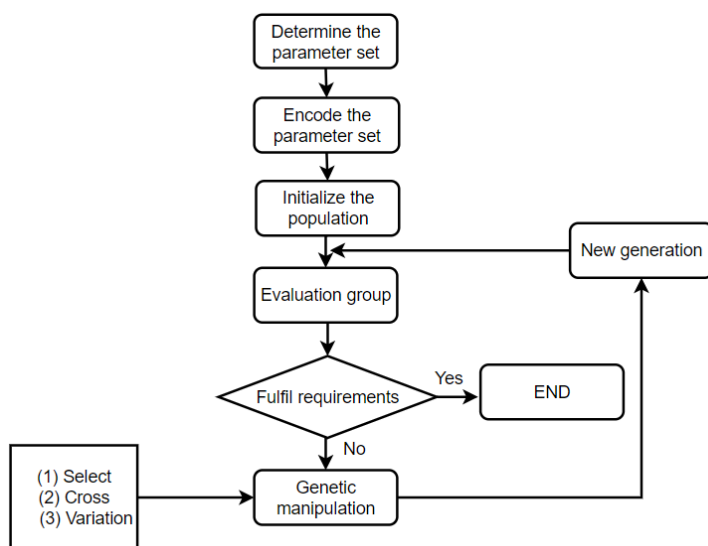


Fig 5: Genetic algorithm operation flow

3.2 Data Analysis and Construction of Multiple Regression Equations

In the above, orthogonal experiments were carried out to determine the ratio of rock-like materials, and the optimal ratio problem can be transformed into a multi-objective optimization problem of rock-like materials. This paper studies the data in Table III and analyzes the quantitative relationship between the proportioning factors and each parameter.

3.2.1 Analysis of variance and range

In this paper, the data in Table III is tested by F, and the squared variance and the squared error of each factor are compared to determine whether the effect of each factor is abnormally obvious. Suppose the experimental results are y_1, y_2, \dots, y_{25} and the experimental results are independent of each other and obey a normal distribution, that is, $y_i \sim N(\mu_i, \sigma)$ ($i = 1, 2, \dots, n$). This paper makes the assumption $H_0: \mu_1 = \mu_2 = \dots = \mu_n$ as a significance assumption. The calculation process is as follows.

$$S_T = \sum_{i=1}^n (y_i - \bar{y})^2 \quad (12)$$

$$= \sum_{i=1}^n y_i^2 - \frac{T^2}{n}$$

$$S_j = t \sum_{i=1}^r (\bar{K}_{ij} - \bar{y})^2 \quad (13)$$

$$= \frac{1}{t} \sum_{i=1}^r K_{ij}^2 - \frac{T^2}{n}$$

In the above formulas,

$$\bar{y} = \frac{1}{n} \sum_{i=1}^n y_i; T \quad (14)$$

$$= \sum_{i=1}^n y_i$$

$$K_{ij} = \sum_{k=1}^t y_{ij,k}; \bar{K}_{ij} = \frac{K_{ij}}{t} \quad (15)$$

S_j is the sum of squared deviations of the j th column factor, K_{ij} is the statistical parameter of the factor j at the i level, and $y_{ij,k}$ is the k th experimental result of the factor j at the i level. The following conclusions can be drawn.

$$S_T = \sum_{j=1}^m S_j \quad (16)$$

Through calculation, the results of variance analysis are shown in Table IV.

TABLEIV. ANALYSIS OF VARIANCE RESULTS

	Saliency	Water-to-paste ratio	Iron content	Sand content
σ_c	F	87.06	13.52	3.68
	P	<0.001	0.007	0.036
	Saliency	$\alpha \leq 0.001$	$0.001 < \alpha \leq 0.01$	$0.01 < \alpha \leq 0.05$
σ_t	F	97.16	28.16	3.51
	P	<0.001	0.004	0.049
	Saliency	$\alpha \leq 0.001$	$0.001 < \alpha \leq 0.01$	
τ_f	F	72.22	5.67	0.09
	P	<0.001	0.006	0.99
	Saliency	$\alpha \leq 0.001$	$0.001 < \alpha \leq 0.01$	
E	F	9.11	1.20	3.62
	P	0.001	0.376	0.037
	Saliency	$\alpha \leq 0.001$	$0.001 < \alpha \leq 0.01$	$0.01 < \alpha \leq 0.05$
v	F	42.31	4.81	0.97
	P	<0.001	0.013	0.651
	Saliency	$\alpha \leq 0.001$	$0.01 < \alpha \leq 0.05$	
φ	F	3.15	3.57	2.72
	P	0.061	0.032	0.087
	Saliency		$0.01 < \alpha \leq 0.05$	
c	F	114.41	24.68	3.42
	P	<0.001	0.007	0.052

Saliency	$\alpha \leq 0.001$	$0.001 < \alpha \leq 0.01$	$0.01 < \alpha \leq 0.05$
----------	---------------------	----------------------------	---------------------------

In this paper, the range calculation is performed on the data in Table III, that is,

$$R_i = \max(t_{ij}^1, t_{ij}^2, t_{ij}^3) - \min(t_{ij}^1, t_{ij}^2, t_{ij}^3) \quad (17)$$

Through calculation and analysis combined with the variance results shown in Table IV, it can be concluded that the water-to-gypsum ratio, iron content and sand content have a quantitative relationship for rock-like materials.

3.2.2 Linear optimization of multiple factors

According to the results listed above, it can be seen that the three proportioning factors have a certain relationship with the mechanical parameters. In this paper, it is regarded as a linear optimization problem with multiple factors, and the experiment is fitted and compared by establishing a multiple regression linear equation.

Let the number of dependent variables be i , the dependent variables be y_1, y_2, \dots, y_i , and each factor in the matching process is set as i independent variables, namely x_1, x_2, \dots, x_i , and the regression equation is constructed as follows.

$$y_{(1,2,\dots,i)} = b_0 + b_1x_1 + b_2x_2 + \dots + b_ix_i \quad (18)$$

From it, b_i is the regression parameter.

After performing multiple regression on each parameter, the regression equation of each parameter can be obtained, as shown in Table V.

TABLEV. Multiple regression parametric equation table

Parameter	Multiple regression equation
σ_c	$y_1 = 47.090 - 63.338x_1 + 0.9373x_2 - 0.001042x_3$
σ_t	$y_2 = 2.7698 - 3.74x_1 + 0.0842x_2 + 0.0010x_3$
τ_f	$y_3 = 19.8462 - 32.0347x_1 + 0.3664x_2 - 0.0001x_3$
E	$y_4 = 24.0126 + 28.648x_1 + 0.0132x_2 - 0.0035x_3$
ν	$y_5 = -0.5636 + 1.288x_1 - 0.002x_2 - 0.0001x_3$
φ	$y_6 = 61.9274 - 3.92x_1 - 0.2302x_2 - 0.00094x_3$
c	$y_7 = 6.3112 - 8.66x_1 + 0.1533x_2 - 0.0001x_3$

3.3 Optimization algorithm model construction

Through the established multiple regression equation, the experimental value of the target parameter is solved through the optimization algorithm, that is, the optimal solution of the proportioning coefficient is obtained. In this paper, multivariate linear optimization is carried out by establishing an optimization algorithm model.

First, the objective function of the optimization algorithm should be determined. Assume and define 7 fitting formulas: $\sigma_c^*, \sigma_t^*, \tau_f^*, E^*, v^*, \varphi^*, c^*$; define the experimental values of parameters as: $\sigma_c^l, \sigma_t^l, \tau_f^l, E^l, v^l, \varphi^l, c^l$; substituting the above parameters into the empirical objective function formula (19) and empirical constraint formula (20), the optimization algorithm can be obtained. Objective function formula (21) and constraint formula (22):

$$\text{inf}(x) = \sum_{i=1}^n \frac{|y_i^{\text{lab}} - y_i^*|}{y_i^{\text{lab}}} \quad (19)$$

$$a_j \leq X_j \leq b_j \quad (1 \leq j \leq k) \quad (20)$$

$$\begin{aligned} \text{minf}(x) = & \frac{|\sigma_c^l - \sigma_c^*|}{\sigma_c^l} + \frac{|\sigma_t^l - \sigma_t^*|}{\sigma_t^l} + \frac{|\tau_f^l - \tau_f^*|}{\tau_f^l} \\ & + \frac{|E^l - E^*|}{E^l} + \frac{|v^l - v^*|}{v^l} + \frac{|\varphi^l - \varphi^*|}{\varphi^l} \\ & + \frac{|c^l - c^*|}{c^l} \end{aligned} \quad (21)$$

$$\begin{aligned} 0.46 & \leq X_1 \leq 0.54 \\ 2\% & \leq X_2 \leq 4\% \\ 14.3\% & \leq X_3 \leq 23.8\% \end{aligned} \quad (22)$$

As shown in Figure 6, the running process of the optimization algorithm is:

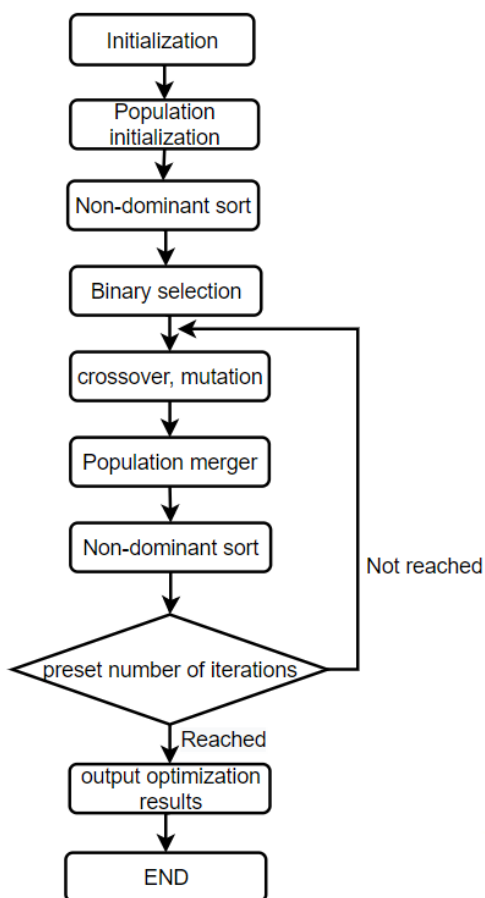
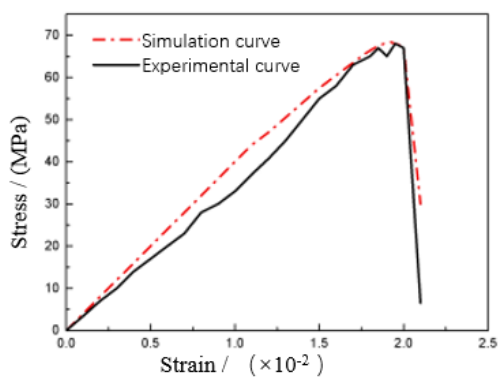
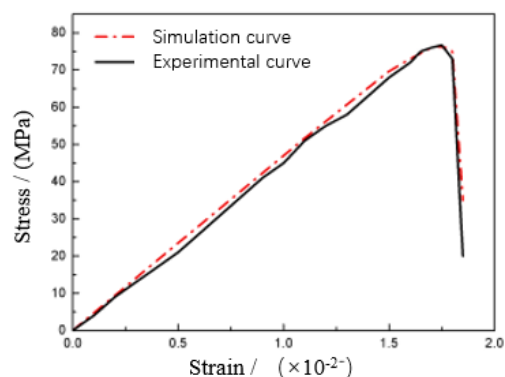


Fig 6: Optimization algorithm operation flow

3.4 Optimal Algorithm Results Verification



(1)



(2)

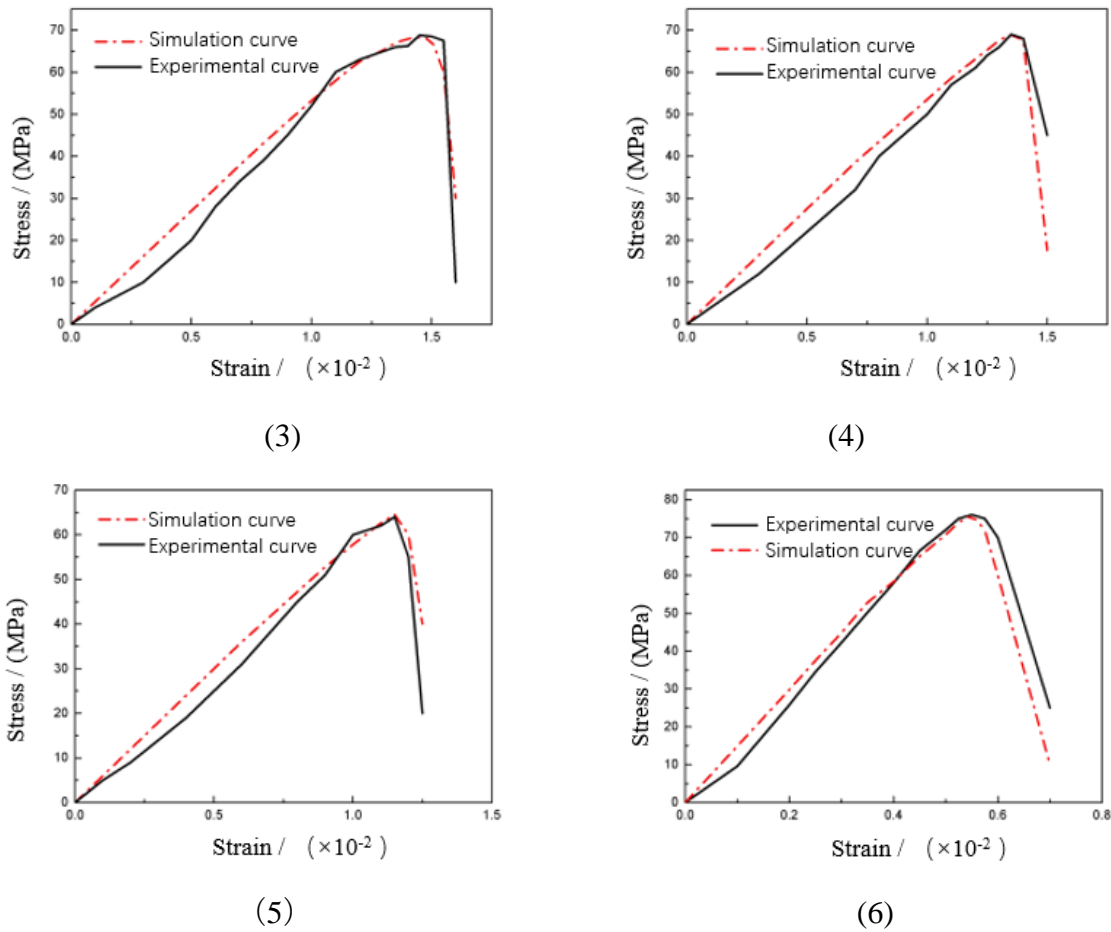


Fig 7: Simulation diagram

After 6 simulation experiments, the results are shown in Figure 7. It can be clearly seen that the simulation results of the algorithm are almost the same as the experimental curves. The simulated data and experimental data are derived and substituted into the relative error formula (23) for calculation.

$$y = \frac{|x^{avg} - x^{tar}|}{x^{avg}} \quad (23)$$

From it, x is the independent variable, y is the relative error, x^{avg} is the mean value of mechanical parameters, and x^{tar} is the simulation parameter value. The error comparison results are shown in Table VI.

TABLEVI. Error comparison result

Parame ters	Target value	Average value	Standard deviation	Coefficient of variation	Relative error
σ_c /Mpa	15	15.06	0.008	<0.001	0.52
σ_t /Mpa	1.00	1.003	<0.001	<0.001	0.26
τ_f /Mpa	3.6	3.517	0.013	0.003	2.04
E/Gpa	5.2	5.224	0.004	0.001	0.67

$\nu/-$	0.14	0.142	<0.001	<0.001	0.56
$\varphi/^\circ$	58.01	57.99	0.058	<0.001	0.03
c/Mpa	2.3	2.336	0.002	<0.001	1.65
σ_t/σ_c	1-15	1/15.16	0.052	0.004	1.02

It can be seen from the above table that the standard deviation of the mechanical parameters of the indoor physical experiment is kept below 0.6, and the coefficient of variation is kept below 1.25. It can be seen that the dispersion of the simulation results is not large and relatively stable. Therefore, the proportioning optimization algorithm designed in this paper has good performance. reference meaning.

IV. PREDICTION OF MECHANICAL PROPERTIES OF PROPORTIONING MATERIALS

4.1 Prediction Principle

In order to better predict the shear resistance of rock and soil, the shear strength prediction of rock-like joints is carried out in this paper after the ratio optimization. This prediction uses BP neural network for prediction, and its network structure is shown in Figure 8.

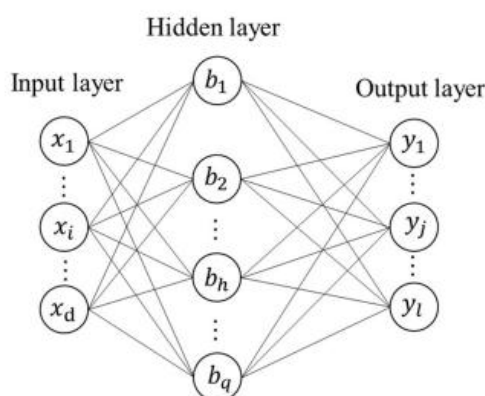


Fig 8: Neural network structure diagram

This paper introduces the empirical formula[10]that is widely used in engineering as follows.

$$\tau_p = \sigma_n \cdot \tan \left(\phi_b + JRC \cdot \log \frac{JCS}{\sigma_n} \right) \quad (24)$$

Among it, JRC is the roughness of the joint surface, JRC is the compressive strength of the joint surface, σ_n is the normal stress, and ϕ_b is the internal friction angle.

The three-dimensional topography function introduced into the rock joint surface[14] is as follows.

$$A_{\theta^*} = A_0 \left(\frac{\theta_{max}^* - \theta^*}{\theta_{max}^*} \right)^c \quad (25)$$

Among it, A_0 is the ratio of the shear surface area to the total area, θ_{max}^* is the maximum effective shear inclination angle in the shear direction, and C is the roughness parameter value.

The shear strength model with the introduction of 3D topography parameters is as follows.

$$\tau_p = \sigma_n \cdot \tan\left[\phi_b + \left(\frac{\theta_{max}^*}{A_0}\right)^{1.18 \cos \alpha} + e^{\frac{-\theta_{max}^* \cdot \sigma_n}{9A_0 C \cdot \sigma_t}}\right] \cdot (1) \quad (26)$$

Introduced, the shear strength model proposed by Xia Caichu et al.[15] is as follows.

$$\tau_p = \sigma_n \cdot \tan\left[\phi_b + \frac{4A_0\theta_{max}^*}{C + 1} + e^{\frac{-\theta_{max}^* \cdot \sigma_n}{9A_0(1+C) \cdot \sigma_t}}\right] \cdot (1) \quad (27)$$

From the empirical formulas and models introduced above, it can be found that there is a strong nonlinear relationship between shear strength and related elements. The neural network can handle a variety of nonlinear mapping capabilities, so this paper uses neural networks to prepare to find their internal relationship.

4.2 Prediction Principle Model Building

First determine the topology optimization structure. In this paper, the cross-validation algorithm is used to determine the neural network topology.

After verification, it is found that in the two-dimensional shear strength neural network, when the network structure is two hidden layers, and the number of neurons is 12 and 6, the network model ANN is 4-12-6-1, and the effect is optimal. At this time, MSE=0.63, and the correlation coefficient is 0.95.

$$\tau_p = f(JRC, JCS, \sigma_n, \phi_b) \quad (28)$$

When the calculation formula of the reconstructed input parameters is formula 26, the two hidden neurons are 27 and 14, and the optimal network model ANN is 4-24-16-1. At this time, MSE=0.51, and its correlation coefficient is 0.94.

$$\tau_p = f(JRC, JCS, \sigma_n, \sigma_n, \phi_b) \quad (29)$$

When the input parameter calculation formula is formula 28, the two hidden elements are 22 and 16 respectively, the optimal, the network model ANN is 4-22-16-1, at this time MSE=0.445, the correlation coefficient is 0.91.

$$\begin{aligned} \tau_p & \\ &= f(A_0, C, \theta_{max}^*, \sigma_t, \sigma_n, \phi_b) \end{aligned} \quad (30)$$

When the input parameter calculation formula is formula 29, the two hidden elements are 248 and 16, respectively, the optimal, the network model ANN is 4-26-14-1, at this time MSE=0.223, the correlation coefficient is 0.97.

$$\begin{aligned} \tau_p = f(A_0, \theta_{max}^* / (C & \\ + 1), \sigma_n / \sigma_t, JCS, \sigma_n, \phi_b) & \end{aligned} \quad (31)$$

After simulation training and testing, the test model is optimized under the Adam and RMSprop optimization algorithms.

4.3 Test results and Conclusions

After calculation, it is found that in the two-dimensional shear strength neural network model, the correlation coefficients of the ANN 4-12-6-1 and ANN 4-24-16-1 test sets are 0.99 and 0.98, respectively, and the correlation is very high. The mean relative errors were 14% and 18%. A model with an ANN of 4-12-6-1 is more concentrated, and the expected value of the normal distribution tends to 0. It can be shown that the use of element data input can help the extraction of neural network features.

The correlation coefficients of the three-dimensional shear strength neural network models ANN: 4-22-16-1 and ANN: 4-48-16-1 test sets are both 0.985; the average relative errors are 11% and 12%, respectively. However, the steps of ANN 4-22-16-1 are relatively more concentrated, so it can be concluded that the original input parameters can show better performance.

V. CONCLUSION

In this paper, through the preparation of rock materials, an orthogonal experimental plan and indoor simulation experiments are carried out to find out the factors that affect the parameters of rock mechanical properties. And using the neural network to analyze its performance, the following conclusions can be drawn.

(1) During uniaxial compression, Brazilian splitting, and direct shear tests, it was found that the prepared rock samples exhibited high brittleness and began to plasticize as the pressure increased.

(2) In the process of ratio optimization, multiple regression equations are established and genetic algorithm evolution is carried out. Experiments show that the error is less than 2%, and the discrete degree of the simulated results is not large and relatively stable. Therefore, the proportioning optimization algorithm designed in this paper has a good reference significance.

(3) When using neural network to predict mechanical properties, the topology optimization structure and neural network model established in this paper analyze and predict different shear strength models, and the average relative error is small. The results show that the use of element data input can help the extraction of

neural network features and the original input parameters can show better performance.

ACKNOWLEDGEMENTS

2021 National Undergraduate Science and Technology Innovation Program(Num.41572297).

REFERENCES

- [1] M. Prudencio and M. Van Sint Jan. Strength and failure modes of rock mass models with non-persistent joints. *International Journal of Rock Mechanics and Mining Sciences*, 2007, 44(6): 890-902.
- [2] Lin Haifei, Yang Erhao, Zhao Pengxiang, ZhuoRisheng, Zhao Bo. Multiple linear regression model of mechanical properties of rock-like materials. *Journal of Xi'an University of Science and Technology*, 2018,38(03):351-359.
- [3] Su Haijian, GuoQingzhen, Jing Hongwen, Hu Chenggong. Research on mechanical properties of rock mass with built-in rough joints based on 3D printing. *Chinese Journal of Mining and Safety Engineering*, 2021, 38(04): 840-846.
- [4] Huang Yanhua, Yang Shengqi, Liu Xiangru. Experimental and numerical simulation of mechanical properties of rock-like materials. *Experimental Mechanics*, 2014, 29(02): 239-249.
- [5] Cao YJ, Shen WQ, Shao JF, Wang W.. A multi-scale model of plasticity and damage for rock-like materials with pores and inclusions. *International Journal of Rock Mechanics and Mining Sciences*, 2021, 138.
- [6] Pi Zizi, Zhou Zilong, Li Xibing, Wang Shaofeng. Digital Image Processing Method for Characterization of Fractures, Fragments, and Particles of Soil/Rock-Like Materials. *Mathematics*,2021,9(8):
- [7] Li Ke. Research on optimization design of green ecological concrete mix ratio. *Central South University of Forestry and Technology*, 2015
- [8] HouQintao, Research on the optimization design of mixture ratio of highway engineering based on neural network. Henan Province, Henan Provincial Highway Engineering Bureau Group Co., Ltd., 2008-12-19.
- [9] Wu Xianguo, Liu Qian, Wang Lei, Chen Bin. Research on multi-objective mix ratio optimization of concrete frost resistance based on LSSVM and GA. *Journal of Shenyang Jianzhu University (Natural Science Edition)*, 2021, 37(03): 393-401.
- [10] Barton N. Review of a new shear-strength criterion for rock joints. *Engineering Geology*, 1973,7(4): 287-332.
- [11] Sayles R S, Thomas T R. The spatial representation of surface roughness by means of the structure function: A practical alternative to correlation. *Wear*, 1977, 42(2): 263-276.
- [12] Feng XT, Katsuyama K, Wang Y, et al. A new direction—Intelligent rock mechanics and rock engineering. *International Journal of Rock Mechanics and Mining Sciences*, 1997,34(1): 135-141. Based on Prediction of shear mechanical properties of rock joints based on BP neural network - 82 –
- [13] Xu Chuanhua, Fang Dingwang, Zhu Shengwu. Neural network method for selecting shear strength parameters of engineering rock mass in slope stability analysis. *Chinese Journal of Rock Mechanics and Engineering*, 2002(06): 858-862.
- [14] Grasselli G, Egger P. Constitutive law for the shear strength of rock joints based on three-dimensional surface parameters. *International Journal of Rock Mechanics and Mining Sciences*, 2003,40(1): 25- 40.
- [15] Tatone B, Grasselli G. A method to evaluate the three-dimensional roughness of fracture surfaces in brittle geomaterials. *Review of Scientific Instruments*, 2009,80(12): 106-181.